Heliyon 10 (2024) e38252

Contents lists available at ScienceDirect

Heliyon

journal homepage: www.cell.com/heliyon

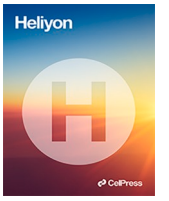

Research article

Inhibitory mechanism on tyrosinase activity of flavonoids from flower buds of *Sophora japonica* L

Yunfeng Ma [a,b,c,1], Chaoyang Zhang [a,1], Jinlin Li [a], Jiayan Xiong [a], Bao-Lin Xiao [a,*]

[a] School of Life Sciences, Henan University, Kaifeng, 475004, China
[b] Institute of Microbial Engineering, Laboratory of Bioresource and Applied Microbiology, Henan University, Kaifeng, 475004, China
[c] Engineering Research Center for Applied Microbiology of Henan Province, Kaifeng, 475004, China

ARTICLE INFO

Keywords:
Tyrosinase
Flavonoids
Sophora japonica L
HPLC fingerprints
Inhibitory activity
Molecular docking
Molecular dynamics simulation

ABSTRACT

The flower buds of *Sophora japonica* L. (FBSJ) have long been applied as Traditional Chinese Medicine (TCM) and functional food in East Asia. In this study, extracts of FBSJ from 11 different locations were analyzed using the HPLC method to establish their HPLC fingerprints. By determining the IC50 on tyrosinase activity, it was discovered that the extract from Kunming, Yunnan Province exhibited the strongest inhibitory activity. Further analysis, including partial least squares regression coefficient analysis and grey correlation analysis, regarded kaempferol, isorhamnetin, and quercetin as the compounds with significant tyrosinase inhibitory activities. To understand the inhibition mechanism of tyrosinase activity, various analytical techniques such as enzymatic kinetic analysis, fluorescence quenching, circular dichroism (CD), molecular docking, and molecular dynamics simulation were employed. The results revealed that quercetin, isorhamnetin, and kaempferol exhibited higher inhibitory activity and binding energy compared with kojic acid, indicating their potential value as natural tyrosinase inhibitors. This research provides a solid theoretical foundation for studying the application and mechanism of flavonoids against tyrosinase in FBSJ.

1. Introduction

Tyrosinase (TYR) serves as a crucial enzyme in melanin synthesis, acting to catalyze tyrosine monophenol and form intermediate products like L-dopa o-diphenol and others [1,2]. Excessive TYR activity has been linked to various pigmentation disorders and the darkening of many foods, and may also plays a role in neurodegeneration associated with Parkinson's disease [3], prompting extensive research into inhibitors of this enzyme. In previous studies, synthetic additives have been used to inhibit enzymatic browning. However, with the increase in consumer health and safety requirements, inhibitors from natural products are beginning to receive extensive attention from researchers [4,5].

Flavonoids, commonly present in plants, comprise a vast group of over 9000 types of compounds with the diphenyl chromone structure primarily binding to sugar to create glycosides, which have a beneficial impact on health [6–9]. Research has demonstrated the protective properties of flavonoids, such as antioxidative and anti-inflammatory effects, as well as cardiovascular healing, anti-obesity, anti-diabetic effects, and more [10–14]. The attention of researchers has recently focused on flavonoids due to their

* Corresponding author.
E-mail address: arixxl@163.com (B.-L. Xiao).
[1] This authors contributed equally to this work.

https://doi.org/10.1016/j.heliyon.2024.e38252
Received 6 May 2024; Received in revised form 18 June 2024; Accepted 20 September 2024
Available online 21 September 2024

non-toxic nature towards tyrosinase, with studies highlighting their efficacy as potential skin whitening agents by inhibiting the tyrosinase enzyme and regulating melanin production [15–17].

Flower buds from *Sophora japonica* L. (FBSJ), commonly used in East Asia as a traditional medicine and functional food, contain various flavonoids like rutin, quercetin, kaempferol, isorhamnetin, narcissoside, nicotiflorin, and genistein [18–21]. The high rutin content, reaching up to 22 % in FBSJ, has led to the cultivation of the plant for rutin extraction purposes [22,23], as potential tyrosinase inhibitors.

However, the analysis of flavonoids in certain plants has revealed both activating and inhibitory effects on tyrosinase, but the identification of compounds with potent tyrosinase inhibitory properties among numerous flavonoids remains a labor-intensive process [24–30]. Fingerprint spectra are a widely recognized method used globally for assessing the quality of Traditional Chinese Medicine (TCM). They can uncover the material foundation of TCM's therapeutic benefits. Additionally, research on the relationship between spectra and effects has been conducted across various fields, origins, harvest times, processing methods, extraction methods, and TCM batches [31–34]. Consequently, an analysis of the HPLC fingerprint was performed, along with an examination of the correlation between common peaks and tyrosinase inhibitory activity to predict the target compounds [35,36].

By evaluating the correlation between fingerprints and the inhibition activity of different extractions, significant components affecting enzyme activity were identified. The inhibitory mechanism was further investigated through enzyme kinetic analysis, circular dichroism (CD), fluorescence quenching, molecular dynamic simulation, and molecular docking. This comprehensive approach aids in uncovering the role of key groups in enzymatic actions, along with comparing the activities of substances with similar structures [37–40].

2. Material and methods

2.1. Materials and instruments

FBSJ of Kaifeng was collected in compus of Henan University in August. FBSJ of other areas werebrought from local places (Table 1). FBSJ was sievedthrough a 200 mesh screen to control the particle size. Tyrosinase was purchased from Bomei Biochemical Co. (Hefei, Anhui Province) and Kuerhuaxue Co. (Hefei, Anhui Province). Rutin, Quercetin, kaempferol, isorhamnetin, genistein, and narcissoside were purchased from Chengdu PureChem-Standard Co. Methanol was chromatographically reagent grade. All other chemicals used in this study were of analytical reagent grade. Acarbose Tablets were purchased from Bayerhealthcare Co.

Waters HPLC (Milford, Massachusetts, USA) equipped with a Waters 1515 pump, a Waters 2707 autosampler, and a Waters UV detector 2489. Multiskan SkyHigh full wavelength Microplate reader (Thermo Fisher Scientific, Massachusetts Waltham, USA).

2.2. Determination of flavonoids in samples and correlation analysis

Accurately 3 g FBSJ powder was weighed and put into a 100 mL round bottom flask, and added by 50 mL of 50 % acetone solution, and heated in 80 °C water bath for 30 min through a heating reflux device; the samples were centrifuged at 3500 r/min for 25 min and the supernatant was collected; 50 mL of pure ethyl acetate was added to the filter residue, and heated in 80 °C water bath for 30 min through a heating reflux device; the samples were centrifuged at 3500 r/min for 25 min and the supernatant was collected; collecting the supernatant twice and dilute it with pure methanol to obtain the extraction solution of FBSJ. And then the extraction solution of FBSJ from different origins repeated the process for the test.

The active ingredients in FBSJ were extracted by 90 % alcohol. Standard flavonoids were dissolved in methanol. The flavonoids in samples were separated using a Waters HPLC. Breeze Software was applied for the data processing. Chromatographic condition 1: Analysis was performed using the Waters high-performance liquid chromatograph with a Waters-C18 column (2) (dimensions: 250 mm × 4.6 mm). Chromatographic separation took place at 30 °C with a flow rate of 1.0 mL min−1, using methanol (A) and 0.05 % phosphoric acid (B) as the solvent. The elution program consisted of the following gradient steps: 0–10 min, 24–40 % (A); 10–20 min,

Table 1
Semi-inhibitory concentration of *S. japonica* extract from different habitats on tyrosinase activity.

Sample source	IC_{50} (mg/mL)
Anhui Bozhou	116.1 ± 2.33
Jilin Changchun	112.4 ± 1.02
Shandong Jining	120.6 ± 1.60
Shandong Rizhao	160 ± 2.67
Anhui Luan	97.19 ± 0.62
Shanxi Jincheng	88.87 ± 0.56
Shandong Taian	86.93 ± 0.66
Hebei Shijiazhuang	129.8 ± 1.78
Henan Xinxiang	82.98 ± 1.44
Yunnan Kunming	45.47 ± 0.96
Henan Kaifeng	107.9 ± 1.52

Values are presented as mean ± SD (n = 3), and significant difference in each column at $p < 0.05$.

40–50 % (A); 20–35 m. The separated flavonoid peaks were identified by comparing the retention time of the standards. Chromatographic Condition 2: The analysis was performed using an Agilent NH_2 column (150 × 4.6 mm, 5 m) on a Waters high-performance liquid chromatograph. The mobile phase consisted of methanol, acetonitrile and water (6:3:1) and 0.4 % formic acid. The flow rate was 0.6 mL/min and the column temperature was maintained at 30 °C. The detection wavelength of the UV detector was 365 nm.

2.3. Peak identification

The mixed standard solution containing the standard solution was injected into the HPLC system for qualitative analysis, and its retention time was recorded, and then each standard solution was injected into the HPLC system for quantitative analysis according to the peak area. Peak identification in samples was confirmed through retention time of different standard flavonoids.

2.4. Enzyme inhibition activity assays

According to the experimental procedure [41], there were partial adjustments made. The 96-well plate was positioned under an ice bath and within a dimly lit area. Inhibitors (50 % ethanol), enzymes (pure water), and substrates were introduced into every well of the plate. Following thorough mixing using a pipette and allowing a 5-min incubation period, the 96-well plate along with the reaction mixture was relocated to a water bath set at 37 °C. Upon a 15-min incubation in darkness, the absorbance was directly quantified at 475 nm utilizing a full wavelength enzyme-linked immunosorbent assay. The experiment was repeated three times, and the average and variance were calculated.

The tyrosinase inhibition rate was expressed as follows:

$$\mathrm{Y}(\%) = \left(1 - \frac{A3 - A4}{A1 - A2}\right) \times 100\%$$

A1 is the blank group: enzyme + buffer, A2 is the blank control group: buffer + buffer, A3 is the sample group: enzyme + inhibitor, A4 is the sample control group: buffer + inhibitor, and Y is the tyrosinase inhibition rate. The IC50 value represented the inhibitor concentration required when the enzyme activity was half inhibited and was used to evaluate the inhibitory activity of the inhibitor on the enzyme.

2.5. Kinetic assay for inhibition action

For the general assay of inhibition action, double-reciprocal Lineweaver-Burk, and the inhibition constant were checked by the second plots of the apparent Km/Vm or 1/Vm versus the concentration of the inhibitor [3].

$$\frac{1}{v} = \frac{K_m}{V_{max}} \frac{1}{[S]} + \frac{1}{[S]}$$

$$v = \frac{V_{max}\,[S]}{K_m\left(1 + \frac{[I]}{K_i}\right) + [S]\left(1 + \frac{[I]}{K_i}\right)}$$

Competitive inhibition:

$$\frac{1}{v} = \frac{K_m}{V_{max}}\left(1 + \frac{[I]}{K_i}\right)\frac{1}{[S]} + \frac{1}{V_{max}}$$

Uncompetitive inhibition:

$$\frac{1}{v} = \frac{K_m}{V_{max}}\frac{1}{[S]} + \frac{1}{V_{max}}\left(1 + \frac{[I]}{K_i}\right)$$

Noncompetitive inhibition:

$$\frac{1}{v} = \frac{K_m}{V_{max}}\left(1 + \frac{[I]}{K_i}\right)\frac{1}{[S]} + \frac{1}{V_{max}}\left(1 + \frac{[I]}{K_i}\right)$$

Mixed inhibition:

$$\frac{1}{v} = \frac{K_m}{V_{max}}\left(1 + \frac{[I]}{K_i}\right)\frac{1}{[S]} + \frac{1}{V_{max}}\left(1 + \frac{[I]}{K_{is}}\right)$$

$$\mathrm{Slope} = \frac{K_m}{V_{max}}\left(1 + \frac{[I]}{K_i}\right)$$

$$Y_{intercept} = \frac{1}{V_{max}}\left(1 + \frac{[I]}{K_{is}}\right)$$

where v is the reaction rate; Vmax stands for the maximum reaction rate; Km stands for the Michaelis-Menten constant, Ki and Kis represent the dissociation constant of the binding inhibitor to free enzyme and enzyme-substrate complex, respectively; [S] stands for substrate concentration. [I] represents the concentration of the inhibitor.

2.6. Fluorescence spectrum analysis

A test to analyze the interaction between tyrosinase and flavonoids in FBSJ was conducted using fluorescence quenching [1]: The method involved placing a mixture of tyrosinase and each solution in water baths at temperatures of 298 K, 304 K, and 310 K for 5 min. The samples were then excited at 280 nm and emitted light within the range of 300–500 nm, with slits set at a width of 5.0 nm. A phosphate buffer solution (PBS) served as the control group. The values of K_{SV}, K_q, and the quenching types were determined using the Stern-Volmer equation [18].

$$\frac{F0}{F} = 1 + K_{sv}[Q] = 1 + K_q\tau_0[Q]$$

$$\lg\frac{F_0 - F}{F} = \lg K_a + n\lg[Q]$$

where F0 and F represent the fluorescence intensity with or without flavonoids, [Q] represents the concentration of quencher, and τ0 (10^{-8} s) is the lifetime of the fluorophore.

2.7. Circular dichroism (CD) spectrum analysis

Tyrosinase was scanned by CD spectrum, and 1.2 mg/L tyrosinase was mixed with quercetin, kaempferol, and isorhamnetin at 0.3 mg/mL, and then the mixed solution was scanned in the wavelength range of 190–260 nm. Results were analyzed on professional websites (http://dichroweb.cryst.bbk.ac.uk).

2.8. Molecular docking

Molecular docking is a very useful method for evaluating ligand-protein binding ability [42,43]. In this paper, AutoDock4 [44] and MGL Tools 1.5.6 were used for molecular docking, Protein data for tyrosinase (PDB ID: 2Y9W) was obtained from RCSB Protein Data Bank, and compounds were downloaded from PubChem (CID: Quercetin 5280343, Kaempferol 5280863, Isorhamnetin 5281654, Kojic acid 3840). Before docking, edit the protein PDB file, keeping the Chain A and the copper ions, adding hydrogen atoms, and distributing the Gasteiger charge to generate the PDBQT file. The gridcenter of tyrosinase was 1.115, 32.227, 99.473, and the girdbox was 70 70 70. Under the default parameters, the Lamarckian genetic algorithm (LGA) is selected for docking calculation. Finally, the lowest binding energy pattern of the complex was visualized with PyMOL [45].

2.9. Molecular dynamics simulation

The results of docking are used as the initial structure of the simulation, and the gromacs 2023.1 [46,47] is used as the simulation software. Charmm3.6 was selected as the protein and small-molecule force field, the TIP3P model was used to add solvent, and sodium

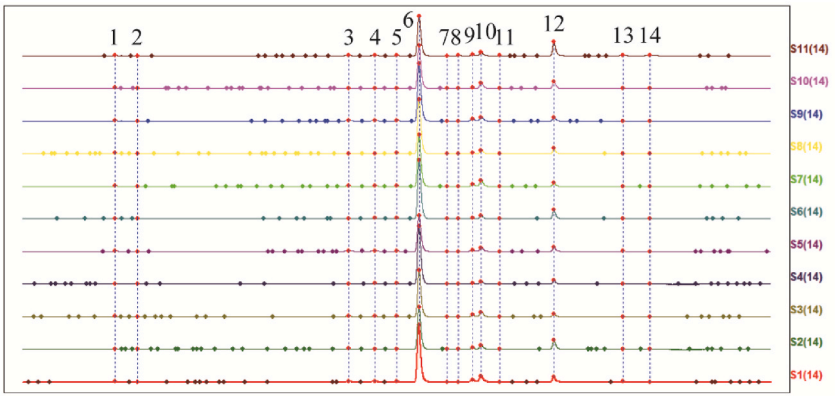

Fig. 1. HPLC fingerprint of FBSJ from different habitats.

ions (Na^{+}) were added to make the system an electric center. The Particle-mesh Ewald algorithm [48,49] was used to calculate electrostatic interactions with a 1.2 Å cutoff. The V-rescale and the Parrinello–Rahman algorithms were applied to couple the temperature and pressure. Energy minimization using the steepest descent algorithm with a tolerance value of 1000 kJ $mol^{-1}nm^{-1}$ in 50, 000 steps, then NVT and NPT equilibrations for 2ns, and finally MD was performed for 100 ns at 300 K temperature and 1 bar pressure.

2.10. Statistical analysis

Results were shown as means ± standard deviation (SD) of three measurements. Statistical analysis was performed using Student's t-test in Excel and a significant difference was statistically considered at the level of $p < 0.05$. Excel was used to calculate the analysis of variance, and the chromatographic fingerprint similarity evaluation system 2012 was used to draw the fingerprint.

3. Results and discussion

3.1. HPLC fingerprint of FBSJ

Every sample was injected three times and the results had no significant differences($p < 0.05$).The HPLC fingerprints of 11 different origins of FBSJ are shown in Fig. 1, which indicates that the common peaks correspond to each other and certain differences in the types and content of compounds they contain. 14 common peaks are labeled with good separation in Fig. 1. By comparing the chromatogram with the reference substance, six chromatographic peaks were identified, as shown in Fig. 2. Among them, peak 6 is rutin, peak 9 is kaempferol 3-O-rutoside, peak 10 is aquaporin, peak 12 is quercetin, peak 13 is kaempferol, and peak 14 is isorhamnetin. The relative standard deviation of the adjusted retention time in the fingerprint spectra of FBSJ from different regions was calculated to be less than 0.25 %, indicating that the retention value was relatively stable, with the relative standard deviation of the peaks area ranging from 16.19 % to 75.88 %, indicating significant differences in compound content.

3.2. IC50 of FBSJ on tyrosinase activity

According to the method[], the semi-inhibitory activity (IC50) of FBSJ extraction on tyrosinase showed that the sample from Yunnan Kunming had the best inhibitory effect on tyrosinase, which indicated that it contained abundant tyrosinase inhibitory active substances. The sample from Shandong Rizhao had the worst inhibitory effect, and there were significant differences in inhibitory effects among samples from different regions, as shown in Table 1.

The partial least squares regression coefficient analysis results showed that there was a negative correlation between peaks 8, 11, quercetin, kaempferol, and isorhamnetin and tyrosinase inhibition ability, with a correlation coefficient $R < -0.2$(Fig. 3). This means that the higher the content of these compounds, the lower the IC50 value, indicating that these compounds have a significant inhibitory effect on tyrosinase. On the contrary, there is a positive correlation between peak 3, narcissoside, and tyrosinase inhibition ability, with a correlation coefficient of $R > 0.2$, indicating that the higher the content of these compounds, the higher the IC50 value. The correlation results by grey relational analysis between the 14 common peaks in FBSJ from different regions and tyrosinase in Table 2 showed that the substances ranked high, such as narcissoside, peak 3, and rutin, had a greater correlation with tyrosinase, indicating that the richer the content of these substances were, the higher the IC50 value was. On the contrary, the lower ranked peaks 4, kaempferol, 11, 8, isorhamnetin, and quercetin have lower correlation with IC50 values, indicating that an increase in the content of these substances can lead to a decrease in IC50 values, which may have a stronger inhibitory effect on tyrosinase. The results are consistent with the partial least squares regression coefficient analysis.

The IC50 results in Table 3 of these four types of flavonoids on tyrosinase showed that their inhibitory effect was better than that of

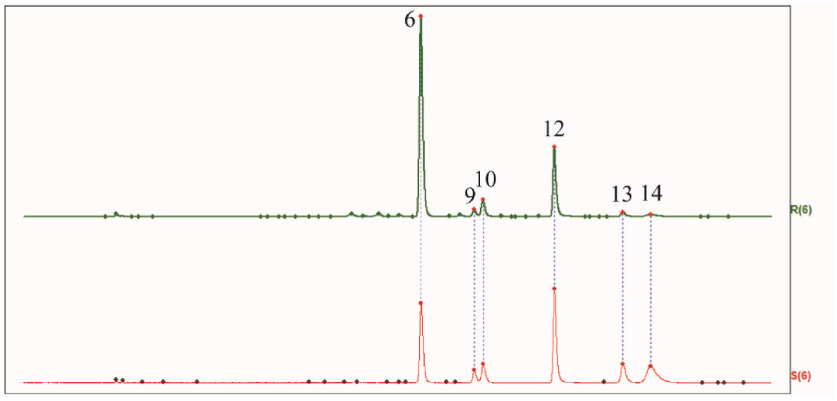

Fig. 2. Control fingerprints of FBSJ (b) control profiles with specimen controls: 6-Rutin; 9-Shanaiol-3-O-rutinoside; 10-Aquaporin; 12-Quercetin; 13-Kaempferol; 14-Isorhamnetin.

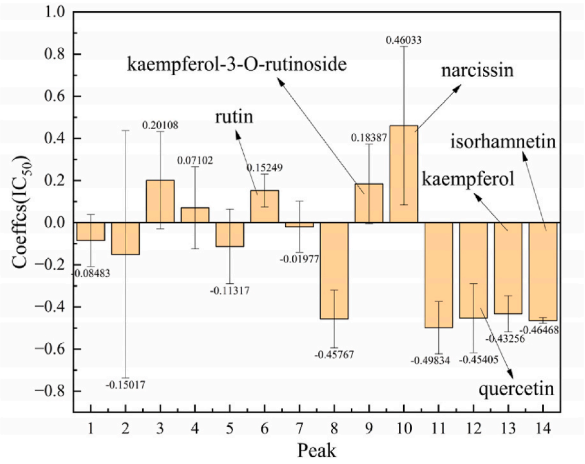

Fig. 3. Partial least squares regression coefficient analysis plot (PLSR).

Table 2
Grey correlation results.

Appraisal items	Correlation degree	Ranking	Appraisal items	Correlation degree	Ranking
Narcissin	0.891	1	Peak 5	0.843	8
Peak 3	0.882	2	Quercetin	0.814	9
Rutin	0.87	3	Isorhamnetin	0.808	10
Peak 2	0.868	4	Peak 8	0.802	11
Peak 1	0.866	5	Peak 11	0.801	12
Peak 7	0.857	6	Kaempferol	0.773	13
Kaempferol-3-o-rutinoside	0.847	7	Peak 4	0.737	14

Significant difference in each column at $p < 0.05$.

Table 3
IC_{50} of quercetin, isorhamnetin, kaempferol and kojic acid.

Standards	$IC_{50}(10^{-5}$ mol/L)
Kaempferol	8.21 ± 1.37
Isorhamnetin	9.64 ± 0.99
Quercetin	7.44 ± 0.76
Kojic acid	17.59 ± 0.51

Significant difference in each column at $p < 0.05$.

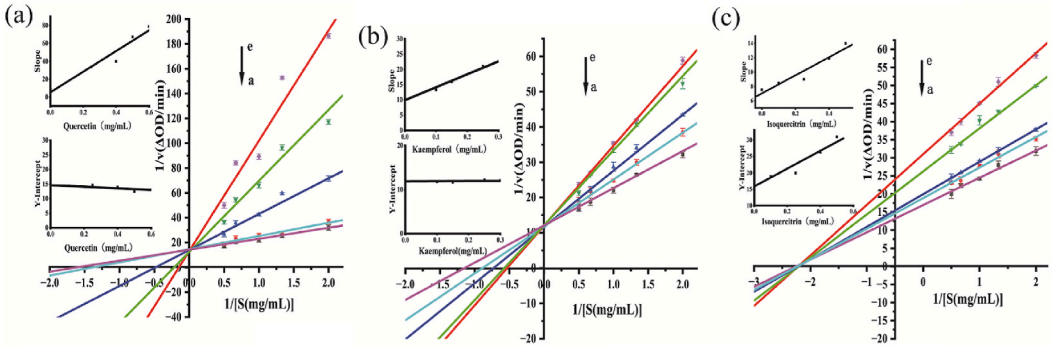

Fig. 4. Kinetic curves of tyrosinase inhibition by quercetin, kaempferol, and isorhamnetin. (a) Quercetin (from 0,0.25, 0.4, 0.5, 0.6 mg/mL; a→e), (b) Kaempferol (from 0, 0.1, 0.15, 0.25, 0.3 mg/mL; a→e), Figure (c) isorhamnetin (from 0, 0.1, 0.25, 0.5 mg/mL; a→d).

traditional tyrosinase inhibitor kojic acid, further confirming the screening results.

3.3. Enzyme inhibition kinetics

To investigate the inhibitory mechanism of flavonoids on tyrosinase, a Lineweaver Burk plot was developed to analyze the inhibitory types of quercetin, kaempferol, and isorhamnosin on tyrosinase. Double reciprocal plots of different concentrations of substrates were obtained based on the enzyme activity reaction rate, which was linear and crossed the second or third quadrant. The results in Fig. 4 indicate that the inhibitory types of quercetin and kaempferol on tyrosinase are competitive because the lines of inhibitors of different concentrations intersect the y-axis and have a constant value of $1/V_{max}$ and the vertical intercept ($1/V_{max}$) and the horizontal intercept ($1\ /K_m$) change simultaneously and linearly, consistent with the reported results [50,51]. The V_{max} value decreases with the increase of the K_m value, as shown in Fig. 4 (a) (b), which means that they compete with the substrate for the active site of the enzyme, thus affecting the enzyme reaction activity. The inhibition type of isorhamnetin and tyrosinase is mixed inhibition, consistent with the reported result [52]. As shown in Fig. 4 (c), all lines intersect in the second quadrant, indicating that isorhamnetin can bind to both free enzymes and enzyme substrate complexes. In addition, the slope and y-intercept quadratic remapping plots are linearly fitted, which indicates that they bind to a certain inhibitory site or type of binding site on tyrosinase.

The K_i and K_{is} values of these three kinds of flavonoids and tyrosinase were calculated according to the formula, which was shown in Table 4. The K_{is} value of isorhamnetin was greater than the K_i value, indicating that its binding ability with tyrosinase was stronger than that of enzyme and substrate.

3.4. Fluorescence quenching of tyrosinase

To investigate the interaction mechanism between flavonoids and tyrosinase, the fluorescence spectra of isorhamnetin, kaempferol, quercetin binding to tyrosinase were measured at three temperatures (298 K, 304 K, and 310 K), and the fluorescence emission spectra of tyrosinase were measured with and without inhibitors. The results in Fig. 5 described that the fluorescence spectra of tyrosinase with isorhamnetin, kaempferol, and quercetin at different temperatures. Tyrosinase had the maximum absorption peak at 345 nm and as the concentration of these inhibitors increased, the fluorescence intensity significantly regularly decreased the energy value, but the emission position didn't shift significantly, which was consistent with the report [52]. This meant that inhibitors had a significant impact on tyrosinase and these inhibitors interacted with tyrosinase to quench its endogenous fluorescence.

There are two types of quenching mechanisms between inhibitors and enzymes: static and dynamic quenching. In static quenching, the K_{sv} value of the inhibitor decreases with increasing temperature, which was opposite to dynamic quenching. According to the Stern-Volmer equation, the K_{sv} values of quercetin, kaempferol and isorhamnetin were calculated at different 298 K, 304 K, and 310 K, as shown in Table 5. These values gradually decreased with increasing temperature, indicating that the quenching mechanisms of quercetin, isorhamnetin, kaempferol were static and as the temperature increased, their K_a values significantly changed, indicating that their interaction with tyrosinase was temperature dependent. As shown in Fig. 5, the Stern Volmer diagram showed good linearity at different temperatures, indicating that the fluorescence quenching type might be single. It can be calculated that K_q of quercetin were 1.44×10^{12}, 1.17×10^{12}, and 1.13×10^{12} L mol^{-1} S^{-1} at 298, 304, and 310 K, K_q of kaempferol were 1.03×10^{12}, 0.83×10^{12}, and 0.73×10^{12}, K_q of isorhamnetin were 0.73×10^{12}, 0.65×10^{12}, and 0.51×10^{12}, respectively. The K_q value was greater than the maximum scattering collision quenching constants of biological molecules (2×10^{10} L mol^{-1} s^{-1}), which indicated that the quenching mechanism is static as well. As mentioned above, these results were mainly due to the quenching effect of the ground state complexes they form on endogenous fluorescence.

The calculations show that the numbers of binding sites (n) for isorhamnetin and kaempferol are both close to 1, which means there is only one type of binding site. However, the number of binding sites for quercetin are close to 2, indicating two or two types of binding sites.

The K_a value indicates the binding ability of the inhibitor with the enzyme. A higher K_a value indicates a stronger binding ability. The results are shown in Table 5. As temperature increased, the binding constant (K_a) of quercetin and kaempferol increased. This suggested that the process of quercetin and kaempferol with tyrosinase is an endothermic reaction.

Subsequently, the van't Hoff equation can be employed to derive the thermodynamic constants of quercetin, kaempferol, and isorhamnetin on tyrosinase, including enthalpy change (ΔH°), free energy change (ΔG°), and entropy change (ΔS°).

$$\log K_a = -\frac{\Delta H^\circ}{2.303RT} + \frac{\Delta S^\circ}{2.303R}$$

$$\Delta G^\circ = \Delta H^\circ T\Delta S^\circ$$

Table 4
Detailed kinetic parameters of tyrosinase by quercetin, kaempferol and isorhamnetine

Compound	K_i(mg/ml)[a]	K_{is}(mg/ml)	Inhibition type
Kaempferol	0.232 ± 0.002	–	Competitive
Isorhamnetin	0.520 ± 0.0005	0.924 ± 0.02	Mixed
Quercetin	0.046 ± 0.0035	–	Competitive

[a] Significant difference in each column at $p < 0.05$. Values are given as means ± SD (n = 3).

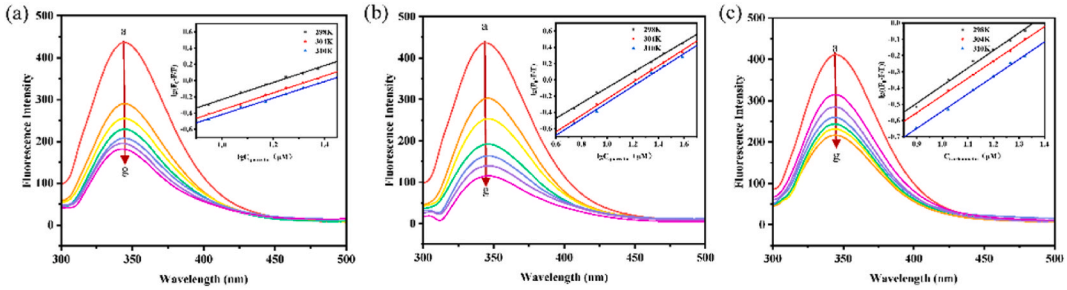

Fig. 5. Fluorescence quenching of tyrosinase by quercetin, kaempferol and isorhamnetin. (a) kaempferol(from 0 → 13.98 × 10^{-5} mol/L; a→g); (b) Quercetin (from 0 → 23.16 × 10^{-5} mol/L; a→g); (c) Isorhamnetin (from 0 → 12.64 × 10^{-5} mol/L; a→g).

Table 5
The thermodynamic parameters of the interaction between quercetin, kaempferol, isorhamnetin, and tyrosinase.

Compound	T (K)	K_{SV} (10^4L·mol^{-1})	K_a (10^5L·mol^{-1})	n	ΔH (KJ mol^{-1})	ΔG (KJ·mol^{-1})	ΔS (J mol^{-1}k^{-1})
Quercetin	298	1.44 ± 0.21	5.12 ± 0.13	1.44	9.12	−3.86 ± 0.05	43.56 ± 3.21
	304	1.17 ± 0.11	5.36 ± 0.21	1.46	±1.3	−4.12 ± 0.02	
	310	1.13 ± 0.15	16.87 ± 0.29	1.61		−4.39 ± 0.02	
Kaempferol	298	1.03 ± 0.04	0.21 ± 0.05	1.08	10.42 ± 1.1	−3.00 ± 0.06	45.03 ± 7.1
	304	0.83 ± 0.1	0.59 ± 0.15	1.22		−3.27 ± 0.03	
	310	0.73 ± 0.02	0.81 ± 0.15	1.27		−3.54 ± 0.05	
Isorhamnetin	298	0.73 ± 0.01	1.83 ± 0.08	1.10	−4.48 ± 2.1	−2.96 ± 0.01	−5.10 ± 1.19
	304	0.65 ± 0.02	1.93 ± 0.21	1.12		−2.93 ± 0.01	
	310	0.51 ± 0.01	1.02 ± 0.18	1.08		−2.90 ± 0.02	

Values are given as means ± SD (n = 3). Significant difference in each column at $p < 0.05$.

in the formula, R is 8.314 J mol^{-1} K^{-1}; T is the experimental temperature.

The values of entropy changes (ΔS°), enthalpy changes (ΔH°), and free energy changes (ΔG°) are presented in Table 5. The negative value of ΔG° indicated that the interaction between tyrosinase and inhibitors occurred spontaneously. The positive value of ΔH° demonstrated that the process of complexing quercetin and kaempferol with the enzyme was an endothermic reaction. The negative value of ΔH° showed that the process of complexing isorhamnetin with tyrosinase was an exothermic reaction. In accordance with the proposed rules by Ross and Subramanian, the observed values of $\Delta S^\circ > 0$ and $\Delta H^\circ > 0$ indicate that the predominant binding forces between quercetin and kaempferol with tyrosinase may be hydrophobic interactions. The values of $\Delta H^\circ < 0$ and $\Delta S^\circ < 0$ demonstrate the presence of hydrogen bonding and van der Waals forces between the enzyme and isorhamnetin.

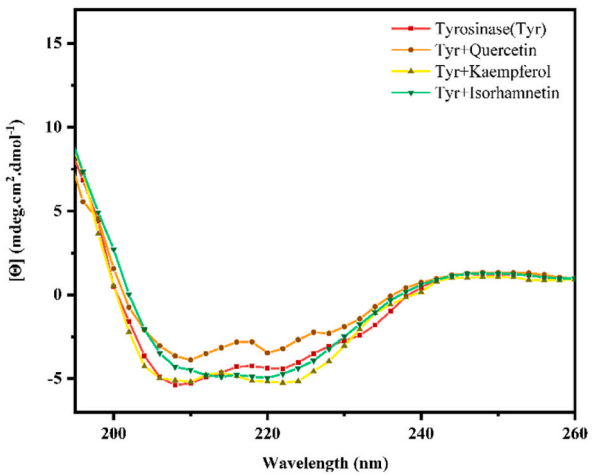

Fig. 6. Circular dichroism of quercetin, kaempferol, isorhamnetin and tyrosinase.

3.5. Circular dichroism of tyrosinase

The changes in the secondary structure of tyrosinase in the presence of different inhibitors were monitored by circular dichroism spectroscopy. As shown in Fig. 6, both negative bands of tyrosinase at 208 nm and 222 nm were altered, suggesting that the α-helix was changed. Because tyrosinase is a 125.31 KDa dimer macromolecular structure, the subunit where the active site is located has 365 amino acid residues, including two in parallel α-helix peptide chains [53], the appearance of a negative band change characteristic of the α-helix in the circular dichroism spectra proves that the binding of the inhibitor to the tyrosinase alters the α-helix, change the folding of the constitutive peptides and reduces stability, ultimately leading to a decrease in the catalytic activity of tyrosinase. In addition, this observation also demonstrates the inhibitor-induced fluorescence quenching of tyrosinase.

3.6. Molecular docking of tyrosinase

To understand the binding mode of these flavonoid inhibitors with tyrosinase, molecular docking was used to simulate the interaction of these flavonoid compounds and kojic acid with tyrosinase, and the optimal binding active component was determined according to the binding energy generated in the docking process. The higher the binding energy was, the more stable and closer the polymers were. The molecular docking analysis of tyrosinase against the preliminarily screened flavonoids showed that kaempferol and tyrosinase had the highest binding energy (−6.08 kcal/mol) from the perspective of energy, as shown in Table 6, followed by quercetin (−5.54 kcal/mol) and isorhamnetin (−5.63 kcal/mol). The binding energy of these small molecules with tyrosinase was similar, and all had good binding effects. The binding energy of tyrosinase positive control kojic acid and tyrosinase was (−4.41 kcal/mol), however, the binding energy of kaempferol-3-o-rutose (−3.88 kcal/mol), narcissoside (−2.89 kcal/mol) and rutin (−2.89 kcal/mol) were poor respectively, which indicated that the binding effect of these three flavonoids with tyrosinase was not as good as that of positive control kojic acid on tyrosinase, The order of binding energy is kaempferol > isorhamnetin > quercetin > kojic acid > kaempferol-3-O-rutoside > narcissoside > rutin, and the results were consistent with the reports [54,55]. This is consistent with the previous partial least squares regression coefficient analysis, grey correlation analysis, and IC50 results for each substance.

The results presented in Fig. 7 demonstrate that the flavonoids with higher binding energies than the positive control kojic acid, were kaempferol, isorhamnetin, and quercetin. Of these, kaempferol and quercetin were hydrogen bonded with HIS85 of tyrosinase, unlike to isorhamnetin. The observed differences in binding modes may be attributed to the type of inhibition, a result that is consistent with previous experimentals. In addition, ASN81, CYS83, HIS85, GLY86 amino acid residues also play an important role in molecular binding. It also shows that the histidine disability that links copper ions plays a crucial role in the molecular docking process, copper chelating six residues (HIS61, HIS85, HIS94, HIS259, HIS263, HIS296) in tyrosinase constituting its active center, as well as a special three-dimensional structure. From the docking results, especially four residues (HIS61, HIS94, HIS259, HIS263) form the binding selectivity, which may limit the rotational freedom of the flavonoids side chain. Three flavonoids contain a large amount of hydrophobic forces around them, as shown in Fig. 7(a–c). However, the binding between kojic acid and tyrosinase has very little hydrophobic force, which may be the reason why these flavonoids have better tyrosinase inhibitory activity than kojic acid, consistent with the report [51].

3.7. Molecular dynamics simulation of tyrosinase

Molecular dynamics simulations were performed on the docking results and analyzed, as shown in Fig. 8. RMSD analysis of the simulation trajectories in Fig. 8a showed that all systems reached equilibrium after 10 ns, with small fluctuations around 0.2, and the isorhamnetin showing abnormal small fluctuations in the middle of the range from 38 to 50 ns, and then reaching a steady state. Overall, the four systems reached equilibrium, and the four conjugates were able to stably exist. During the simulation process of four systems, RMSF analysis of proteins (Fig. 8b) revealed significant fluctuations in amino acid residues located at 72–77, 245–251, and 319–331, which suggested that these sites were common binding sites of inhibitors, among which, the system bound to isorhamnetin was significantly different at 248, quercetin was different at 74, and kaempferol and kojic acid had large fluctuations at 76. These results suggest that different inhibitors also have different binding sites, which in turn affect the conformation of proteins. Rg reflects the compactness of the protein. By analyzing the radius of gyration of the proteins (Fig. 8c) during the simulation, except for kaempferol, the Rg of protein in other systems fluctuated at 2.08 nm after the system was equilibrated, and the fluctuation of kaempferol was slightly larger. During the whole simulation, the Rg value of the quercetin complex showed a gradual downward trend, and in general, the quercetin complex was more closely structured. Consistent with SASA (Fig. 8d). By analyzing the energy change of interaction between inhibitors and proteins in the simulation process (Fig. 8f), it is found that the energy of kojic acid and protein interaction is stable, quercetin and kaempferol have certain fluctuations, the interaction is strong, and isorhamnetin fluctuates the most. Combined with the analysis of the centroid distance between the protein and the inhibitor (Fig. 8e), it was further confirmed that the distance between isorhamnetin and the protein fluctuated greatly, and combined with the previous results, it was speculated that there may be multiple forms of isorhamnetin binding to tyrosine.

4. Conclusion

The current research has validated the unique fingerprint patterns of flavonoids in S. japonica across diverse geographical locations. From the evaluation of the inhibitory rate IC50 of tyrosinase in the extract and the correlation analysis of common peak areas in the fingerprint, three established flavonoids exhibiting significant inhibitory effects were identified: quercetin, isorhamnetin, and

Table 6
Molecular docking evaluation of tyrosinase by flavonoid substances in FBSJ.

Material	Binding energy(kcal/mol)[a]	Interaction residues[b]
Kaempferol	−6.08	ASN-81、CYS-83、HIS-85、GUY-86、GLY-245、ALA-246、ASN-320、ARG-321、GLU-322
Isorhamnetin	−5.63	ASN-81、GLY-86、GLY-245、ASN-320、ARG-321、GLU-322
Quercetin	−5.54	TYR-65、TYR-78、LYS-79、ASN-81、CYS-83、HIS-85
Kojic acid	−4.41	ASN-81、CYS-83、HIS-85、GLU-322
Kaempferol-3-O-rutinose	−3.88	GLU-189、ASP-191、ARG-268、LEU-275、GLY-281、SER-282
Narcissin	−2.89	TYR-65、LYS-79、ASN-81、SER-282、VAL-283、GLU-322
Rutin	−2.89	ASN-260、GLU-322、ALA-323

[a] Significant difference in each column at $p < 0.05$.[b] Obtained by PyMOL.

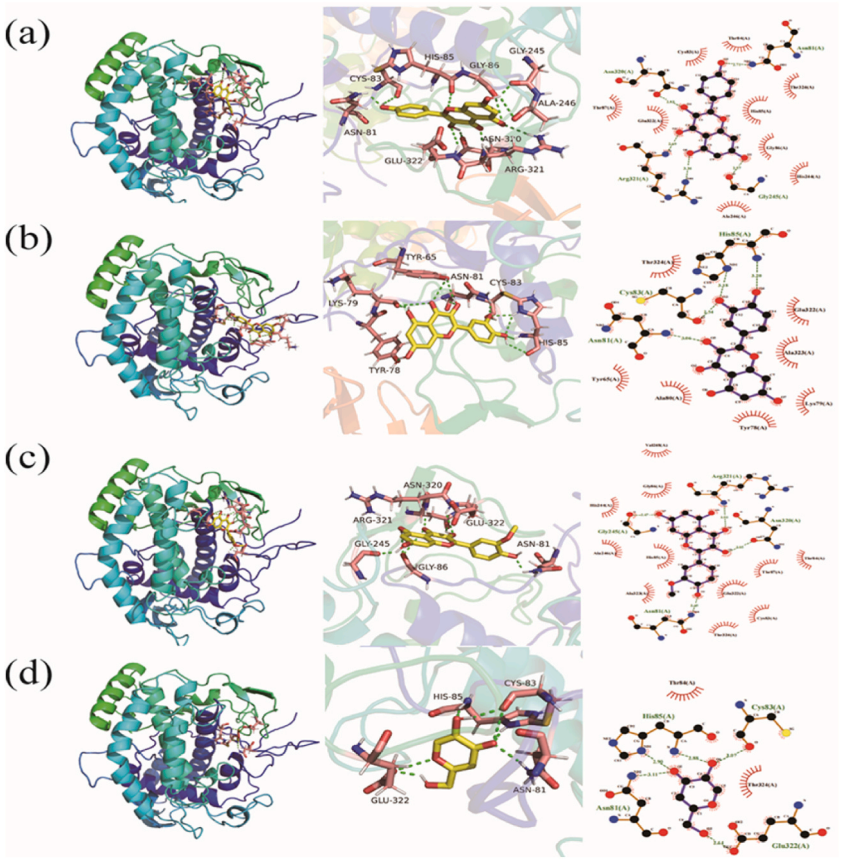

Fig. 7. Molecular docking of the inhibitor and tyrosinase; (a) kaempferol, (b) quercetin, (c) isorhamnetin, (d) kojic acid and tyrosinase. The first and second columns are plotted by PyMOL and the third column is plotted in LigPlot^{+} [56].

kaempferol. These substances demonstrated a higher binding energy compared to kojic acid. The individual testing of these compounds further supported this finding, as they were observed to interact with tyrosinase and induce changes in its secondary structure. Kinetic study showed that kaempferol and quercetin could significantly inhibit the activity of tyrosinase, and the inhibitory types are competitive, the inhibition type of isorhamnetin is mixed inhibition. Both of three quenched the fluorescence of tyrosinase by a static procedure. Unlike quercetin and kaempferol, the binding process of isorhamnetin is accompanied and release heat, while the main binding force of isorhamnetin to tyrosinase is a combination of hydrogen bonding, hydrophobic forces and van der Waals forces, and that of quercetin and kaempferol is hydrophobic forces. Molecular docking and dynamics simulations yielded consistent outcomes, affirming the superior tyrosinase inhibitory activity of these compounds over kojic acid and highlighting their potential as valuable natural inhibitors of tyrosinase.

Data availability

Data will be made available on request.

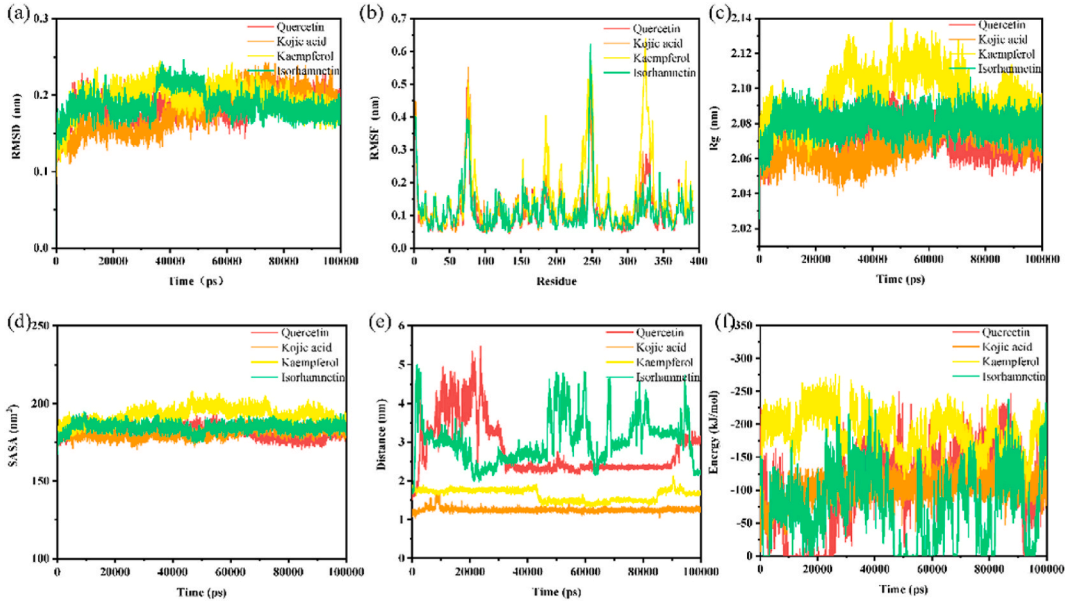

Fig. 8. Molecular dynamics simulations of the inhibitor and tyrosinase. The plot of (a)RMSD, (b)RMSF, (c)Rg, (d) SASA, (e) Distance and (f) Energy of the inhibitor and tyrosinase during simulations.

CRediT authorship contribution statement

Yunfeng Ma: Writing – original draft, Software, Investigation, Formal analysis, Conceptualization. **Chaoyang Zhang:** Writing – original draft, Validation, Software, Investigation, Data curation, Conceptualization. **Jinlin Li:** Validation, Investigation, Formal analysis. **Jiayan Xiong:** Validation, Software, Investigation, Formal analysis. **Bao-Lin Xiao:** Writing – review & editing, Writing – original draft, Supervision, Project administration, Methodology, Funding acquisition, Formal analysis, Data curation, Conceptualization.

Declaration of competing interest

The authors declare that they have no known competing financial interests or personal relationships that could have appeared to influence the work reported in this paper.

Acknowledgment

This research was funded by the National Natural Science Foundation of China, grant number (32161143021), Henan University Research Fund (SYLYC2022104), and the Henan Province Major Research Fund of Public Welfare (No. 201300110900).

References

[1] Y. Lu, Y. Xu, M.-T. Song, L.-L. Qian, X.-L. Liu, R.-Y. Gao, R.-M. Han, L.H. Skibsted, J.-P. Zhang, Promotion effects of flavonoids on browning induced by enzymatic oxidation of tyrosinase: structure–activity relationship, RSC Adv. 11 (2021) 13769–13779.
[2] X. Lai, H.J. Wichers, M. Soler-Lopez, B.W. Dijkstra, Structure and function of human tyrosinase and tyrosinase-related proteins, Chem. Eur J. 24 (2018) 47–55.
[3] D. Şöhretoğlu, S. Sari, B. Barut, A. Özel, Tyrosinase inhibition by some flavonoids: inhibitory activity, mechanism by in vitro and in silico studies, Bioorg. Chem. 81 (2018) 168–174.
[4] B. Gasowska-Bajger, H. Wojtasek, Reactions of flavonoids with o-quinones interfere with the spectrophotometric assay of tyrosinase activity, J. Agric. Food Chem. 64 (2016) 5417–5427.
[5] K.Y. Vasantha, C.S. Murugesh, A.P. Sattur, A tyrosinase inhibitor from *Aspergillus niger*, Journal of Food Science and Technology-Mysore 51 (2014) 2877–2880.
[6] Z. Zhang, M. Wang, S. Xing, C. Zhang, Flavonoids of Rosa rugosa Thunb. inhibit tumor proliferation and metastasis in human hepatocellular carcinoma HepG2 cells, Food Sci. Hum. Wellness 11 (2022) 374–382.
[7] B. Liu, Y. Zhu, Extraction of flavonoids from flavonoid-rich parts in tartary buckwheat and identification of the main flavonoids, J. Food Eng. 78 (2007) 584–587.
[8] D. Grassi, G. Desideri, C. Ferri, Flavonoids: antioxidants against atherosclerosis, Nutrients 2 (2010) 889–902.
[9] U. Prawat, D. Phupornprasert, A. Butsuri, A.-W. Salae, S. Boonsri, P. Tuntiwachwuttikul, Flavonoids from friesodielsia discolor, Phytochem. Lett. 5 (2012) 809–813.
[10] H.-T. Tao, Q. Bin, F.-L. Du, T. Xu, L. Lina, F. Lu, K.-M. Li, L. Wei, The protective effects of cassava (manihot esculenta crantz) leaf flavonoid extracts on liver damage of carbon tetrachloride injured mice, Afr. J. Tradit., Complementary Altern. Med. 12 (2014) 52–56.
[11] Y. Yang, M. Liu, H. Li, Y. Yang, N. Su, Y. Wu, H. Wang, Proteomics analysis of the protective effect of canola (Brassica campestris L.) bee pollen flavonoids on the tert-butyl hydroperoxide-induced EA.hy926 cell injury model, J. Funct.Foods 75 (2020) 104223.

[12] S. Milosavljevic, I. Djordjevic, B. Mandic, V. Tesevic, M. Stankovic, N. Todorovic, M. Novakovic, Flavonoids of the heartwood of cotinus coggygria scop. Showing protective effect on human lymphocyte DNA, Nat. Prod. Commun. 16 (2021) 1934578X211067289.
[13] K.M.M. Koriem, Review on Flos Arnicae: Phytochemical Screening, Chemical Constituents, and Pharmacological Applications, 2021.
[14] D. Malesev, V. Kuntic, Investigation of metal-flavonoid chelates and the determination of flavonoids via metal-flavonoid complexing reactions, J. Serb. Chem. Soc. 72 (2007) 921–939.
[15] H.A.S. El-Nashar, M.I.G. El-Din, L. Hritcu, O.A. Eldahshan, Insights on the inhibitory power of flavonoids on tyrosinase activity: a survey from 2016 to 2021, Molecules 26 (2021).
[16] R.J. Obaid, E.U. Mughal, N. Naeem, A. Sadiq, R.I. Alsantali, R.S. Jassas, Z. Moussa, S.A. Ahmed, Natural and synthetic flavonoid derivatives as new potential tyrosinase inhibitors: a systematic review, RSC Adv. 11 (2021) 22159–22198.
[17] M.A. Baber, C.M. Crist, N.L. Devolve, J.D. Patrone, Tyrosinase inhibitors: a perspective, Molecules 28 (2023).
[18] J. Li, Y. Gong, J. Li, L. Fan, In vitro xanthine oxidase inhibitory properties of Flos Sophorae Immaturus and potential mechanisms, Food Biosci. 47 (2022) 101711.
[19] T.T. Bui, H.T. Nguyen, Ethanolic extract of Sophora japonica flower buds alleviates cognitive deficits induced by scopolamine in mice, Oriental Pharmacy and Experimental Medicine 17 (2017) 337–344.
[20] J.M. Kim, H.S. Yun-Choi, Anti-platelet effects of flavonoids and flavonoid-glycosides from Sophora japonica, Arch Pharm. Res. (Seoul) 31 (2008) 886–890.
[21] N.T. Le, T.P.D. Nguyen, D.V. Ho, H.T. Phung, H.T. Nguyen, Green solvents-based rutin extraction from *Sophora japonica* L, Journal of Applied Research on Medicinal and Aromatic Plants 36 (2023).
[22] E. Horosanskaia, T. Minh Nguyen, T. Dinh Vu, A. Seidel-Morgenstern, H. Lorenz, Crystallization-based isolation of pure rutin from herbal extract of Sophora japonica L, Org. Process Res. Dev. 21 (2017) 1769–1778.
[23] W. Tang, G. Eisenbrand, W. Tang, G. Eisenbrand, Sophora japonica L, Chinese drugs of plant origin: chemistry, Pharmacology, and Use in Traditional and Modern Medicine (1992) 945–955.
[24] K. Jakimiuk, S. Sari, R. Milewski, C.T. Supuran, D. Şöhretoğlu, M. Tomczyk, Flavonoids as tyrosinase inhibitors in in silico and in vitro models: basic framework of SAR using a statistical modelling approach, J. Enzym. Inhib. Med. Chem. 37 (2022) 427–436.
[25] N.K. Lee, K.H. Son, H.W. Chang, S.S. Kang, H. Park, M.Y. Heo, H.P. Kim, Prenylated flavonoids as tyrosinase inhibitors, Arch Pharm. Res. (Seoul) 27 (2004) 1132–1135.
[26] J. Jegal, S.A. Park, K. Chung, H.Y. Chung, J. Lee, E.J. Jeong, K.H. Kim, M.H. Yang, Tyrosinase inhibitory flavonoid from *Juniperus communis* fruits, Biosc. Biotech. Biochem. 80 (2016) 2311–2317.
[27] H.X. Nguyen, N.T. Nguyen, M.H.K. Nguyen, T.H. Le, T.N.V. Do, T.M. Hung, M.T.T. Nguyen, Tyrosinase inhibitory activity of flavonoids from *Artocarpus heterophyllous*, Chem. Cent. J. 10 (2016).
[28] N. Kishore, D. Twilley, A.B. van Staden, P. Verma, B. Singh, G. Cardinali, D. Kovacs, M. Picardo, V. Kumar, N. Lall, Isolation of flavonoids and flavonoid glycosides from *Myrsine africana* and their inhibitory activities against mushroom tyrosinase, J. Nat. Prod. 81 (2018) 49–56.
[29] S.G. Lee, F. Karadeniz, Y. Seo, C.S. Kong, Anti-melanogenic effects of flavonoid glycosides from *Limonium tetragonum* (thunb.) bullock via inhibition of tyrosinase and tyrosinase-related proteins, Molecules 22 (2017).
[30] D. Muhammad, J. Hubert, N. Lalun, J.H. Renault, H. Bobichon, M. Nour, L. Voutquenne-Nazabadioko, Isolation of flavonoids and triterpenoids from the fruits of *alphitonia neocaledonica* and evaluation of their anti-oxidant, anti-tyrosinase and cytotoxic activities, Phytochem. Anal. 26 (2015) 137–144.
[31] W. Li, Y. Zhang, S. Shi, G. Yang, Z. Liu, J. Wang, W. Kang, Spectrum-effect relationship of antioxidant and tyrosinase activity with Malus pumila flowers by UPLC-MS/MS and component knock-out method, Food Chem. Toxicol. 133 (2019) 110754.
[32] Y. Xiao, X. Shan, H. Wang, B. Hong, Z. Ge, J. Ma, Y. Li, Y. Zhao, G. Ma, C. Zhang, Spectrum-effect relationship between HPLC fingerprint and antioxidant of "San-Bai Decoction" extracts, J. Chromatogr. B 1208 (2022) 123380.
[33] Y. Liu, K. Pei, L. He, M. Hu, Spectrum-effect relationship between HPLC fingerprints and inhibitory activity in MUC5AC mucin of pinelliae rhizoma praeparatum cum alumine, Trop. J. Pharmaceut. Res. 21 (2022) 1019–1026.
[34] M. Liu, Y. Wu, S. Huang, H. Liu, J. Feng, Spectrum-effect relationship between HPLC fingerprints and hypolipidemic effect of Curcuma aromatica, Biomed. Chromatogr. 32 (2018) e4220.
[35] C. Liu, C. Ma, J. Lu, L. Cui, M. Li, T. Huang, Y. Han, Y. Li, Z. Liu, Y. Zhang, A rapid method and mechanism to identify the active compounds in Malus micromalus Makino fruit with spectrum-effect relationship, components knock-out and molecular docking technology, Food Chem. Toxicol. 150 (2021) 112086.
[36] K.B. Kang, D.Y. Lee, T.B. Kim, S.H. Kim, H.J. Kim, J. Kim, S.H. Sung, Prediction of tyrosinase inhibitory activities of *Morus alba* root bark extracts from HPLC fingerprints, Microchem. J. 110 (2013) 731–738.
[37] M.H. Fu, W.X. Shen, W.Z. Gao, L. Namujia, X. Yang, J.W. Cao, L.J. Sun, Essential moieties of myricetins, quercetins and catechins for binding and inhibitory activity against α-Glucosidase, Bioorg. Chem. 115 (2021).
[38] T. Ekimoto, M. Ikeguchi, Multiscale molecular dynamics simulations of rotary motor proteins, Biophysical Reviews 10 (2018) 605–615.
[39] C. Chi, X. Li, T. Feng, X. Zeng, L. Chen, L. Li, Improvement in nutritional attributes of rice starch with dodecyl gallate complexation: a molecular dynamic simulation and in vitro study, J. Agric. Food Chem. 66 (2018) 9282–9290.
[40] H.H. Liu, C. Zheng, Z.L. Li, X.Y. Xia, D. Jiang, W. Wang, R.Y. Zhang, X. Xiang, Inhibitory mechanism of phenolic compounds in rapeseed oil on α-amylase and α-glucosidase: spectroscopy, molecular docking, and molecular dynamic simulation, Spectrochim. Acta Mol. Biomol. Spectrosc. 289 (2023).
[41] M.H. Fan, G.W. Zhang, X. Hu, X.M. Xu, D.M. Gong, Quercetin as a tyrosinase inhibitor: inhibitory activity, conformational change and mechanism, Food Res. Int. 100 (2017) 226–233.
[42] L. Lu, X. Zhang, Y. Kang, Z. Xiong, K. Zhang, X. Xu, L. Bai, H. Li, Novel coumarin derivatives as potential tyrosinase inhibitors: synthesis, binding analysis and biological evaluation, Arab. J. Chem. 16 (2023) 104724.
[43] S. Tabassum, S. Ahmad, K. ur Rehman Khan, B. Ali, F. Usman, Q. Jabeen, M. Sajid-ur-Rehman, M. Ahmed, H. Muhammad Zubair, L. Alkazmi, G. El-Saber Batiha, Q.-u. Zaman, A. Basit, Chemical profiling and evaluation of toxicological, antioxidant, anti-inflammatory, anti-nociceptive and tyrosinase inhibitory potential of Portulacaria afra using in-vitro, in-vivo and in-silico studies, Arab. J. Chem. 16 (2023) 104784.
[44] G.M. Morris, R. Huey, W. Lindstrom, M.F. Sanner, R.K. Belew, D.S. Goodsell, A.J. Olson, AutoDock4 and AutoDockTools 4: automated docking with selective receptor flexibility, J. Comput. Chem. 30 (2009) 2785–2791.
[45] S. Yuan, H.C.S. Chan, Z. Hu, Using PyMOL as a platform for computational drug design, WIREs Computational Molecular Science 7 (2017) e1298.
[46] D. Van der Spoel, E. Lindahl, B. Hess, G. Groenhof, A.E. Mark, H.J.C. Berendsen, GROMACS: fast, flexible, and free, J. Comput. Chem. 26 (2005) 1701–1718.
[47] M.J. Abraham, T. Murtola, R. Schulz, S. Páll, J.C. Smith, B. Hess, E. Lindahl, GROMACS: high performance molecular simulations through multi-level parallelism from laptops to supercomputers, SoftwareX 1–2 (2015) 19–25.
[48] T. Darden, D. York, L. Pedersen, Particle mesh Ewald: an N·log(N) method for Ewald sums in large systems, J. Chem. Phys. 98 (1993) 10089–10092.
[49] U. Essmann, L. Perera, M. Berkowitz, T. Darden, S.H. Lee, L. Pedersen, A Smooth Particle Mesh Ewald Potential, 1995.
[50] Y.-L. Xue, T. Miyakawa, Y. Hayashi, K. Okamoto, F. Hu, N. Mitani, K. Furihata, Y. Sawano, M. Tanokura, Isolation and tyrosinase inhibitory effects of polyphenols from the leaves of persimmon, Diospyros kaki, J. Agric. Food Chem. 59 (2011) 6011–6017.
[51] M. Fan, G. Zhang, X. Hu, X. Xu, D. Gong, Quercetin as a tyrosinase inhibitor: inhibitory activity, conformational change and mechanism, Food Res. Int. 100 (2017) 226–233.
[52] Y.-X. Si, Z.-J. Wang, D. Park, H.O. Jeong, S. Ye, H.Y. Chung, J.-M. Yang, S.-J. Yin, G.-Y. Qian, Effects of isorhamnetin on tyrosinase: inhibition kinetics and computational simulation, Biosci. Biotechnol. Biochem. 76 (2012) 1091–1097.
[53] W.T. Ismaya, H.J. Rozeboom, A. Weijn, J.J. Mes, F. Fusetti, H.J. Wichers, B.W. Dijkstra, Crystal structure of Agaricus bisporus mushroom tyrosinase: identity of the tetramer subunits and interaction with tropolone, Biochemistry 50 (2011) 5477–5486.

[54] A. Farasat, M. Ghorbani, N. Gheibi, H. Shariatifar, In silico assessment of the inhibitory effect of four flavonoids (Chrysin, Naringin, Quercetin, Kaempferol) on tyrosinase activity using the MD simulation approach, BioTechnologia, Journal of Biotechnology Computational Biology and Bionanotechnology (2020) 101.
[55] X. Li, J. Guo, J. Lian, F. Gao, A.J. Khan, T. Wang, F. Zhang, Molecular simulation study on the interaction between tyrosinase and flavonoids from sea buckthorn, ACS Omega 6 (2021) 21579–21585.
[56] R.A. Laskowski, M.B. Swindells, LigPlot+: multiple ligand-protein interaction diagrams for drug discovery, J. Chem. Inf. Model. 51 (2011) 2778–2786.